Computer Science and Information Systems 15(3):501–515 https://doi.org/10.2298/CSIS171020019Z

Research on Automatic Identification Technique of CT Image in Lung

Zhijie Zhao[1,2], Cong Ren[1,2], Huadong Sun[1,2], Zhipeng Fan[1,2], and Ze Gao[1,2]

[1] School of Computer and Information Engineering, Harbin University of Commerce, Harbin, 150028, China,
Zhaozj@hrbcu.edu.cn, 1242944210@qq.com, kof97_sun@163.com, fanzhipeng@hrbcu.edu.cn, 1041451358@qq.com
[2] Key Laboratory of Electronic Commerce and Information Processing of Heilongjiang Province

Abstract. Lung cancer has become the world's human cancer disease in the "first killer." In this paper, three aspects of lung CT images were treated. Firstly, based on the CT image preprocessing, the lung parenchyma was segmented by random walk algorithm and the ROI was extracted from the pulmonary parenchyma; Secondly, the 10-dimensional feature vectors of pulmonary nodule ROI were extracted by the gray level co-occurrence matrix algorithm; Finally, support vector machine as a classifier is to identify the pulmonary nodules and the accuracy rate is more than 94%. The experimental results show that the study of automatic CT image recognition can provide some data reference for doctors and play a supporting role in the course of treatment.

Keywords: CT image, image segmentation, ROI extraction, feature extraction, support vector machine.

1. Introduction

According to the survey research shows that cancer has become a major problem affecting human health in the world. Among all types of cancer, lung cancer mortality is higher than other types of cancer mortality. The 2015 global cancer statistics [1] was published in journal of the CA on February 4, 2015. It is expected that in 2012, about 820 million patients worldwide died of cancer, and 14.1 million new cases were found in cancer cases, and there are more cancer patients and cancer deaths in developing countries than in developed countries. At present, lung cancer is the leading cause of death in male patients. In recent years, due to the extreme pollution of the city, a substantial increase in smoking population, lung cancer early difficult to be found by doctors and late difficult to be cured and other factors, the incidence of lung cancer in the population is increasing year by year.

In the world of medical organizations and researchers under the continuous efforts, lung cancer has been greatly improved [2] in the diagnostic methods and treatment levels, and lung cancer patients in the mortality and morbidity has not been improved, there are three main reasons: (1) lung cancer is not only difficult to distinguish in case

characteristics, but also fast to deteriorate; (2) because the early symptoms of lung cancer are not very significant, it is easy to not be found that more than 80% of the sick people have been diagnosed with the condition of the disease in the advanced stage of lung cancer; (3) the current imaging diagnosis relies mainly on the completion of manual reading, however, the increasing image data also poses a great challenge to manual reading. In order to provide effective diagnostic information for doctors, intelligent image processing technology is becoming more and more important [3-5]. Computer aided diagnosis, which is based on machine learning and image processing technology, has gradually become a hotspot in the field of medicine [6]. Computer aided diagnosis based on machine learning mainly includes four aspects: image preprocessing; image segmentation and region of interest (ROI) extraction; feature extraction; selection and classification.

At present, the study of automatic CT images in the lungs has been paid more and more attention. The method of artificial intelligence to identify pulmonary nodules has played a vital role in the medical field. The 96 shape features were extracted by Kim B. C., Yu S. S. and Suk H. I. [7], including the standard deviation, perimeter, circle diameter, area of malignant nodules and benign nodules. The shape feature extracted from the region of interest form a matrix, and classified by SVM. The accuracy rate is 95.5% and the specificity is 94.4%. The 200 depth features extracted from the LIDC database in a 5-layer denoising encoder were extracted by Kumar D., Wong A. and Clausi D. A. [8], which was divided into benign pulmonary nodules and malignant pulmonary nodules using decision trees, the average accuracy and sensitivity were 75.01% and 83.35%. Ashis Kumar Dhara, Anirvan Dutta and Sudipta Mukhopadhyay et al. [9] proposed an effective classification program to distinguish between benign and malignant pulmonary nodules, which are classified by shape, edge and texture to assist radiologists Diagnosis of lung cancer and improve the accuracy of classification.

2. Segmentation of Pulmonary Parenchyma in CT Images Based on Random Walk Algorithm

Y Ozen and Wang Bing et al. [10-11] proposed an automatic segmentation of lung CT with random walk algorithm. In this paper, the CT images of pulmonary parenchyma were segmented interactively based on the random walk algorithm. Firstly, according to the characteristics of CT images in medical images, the seeds of the foreground were labeled in the pulmonary parenchyma, and the seeds of the background were labeled in the thorax, heart, trachea and background area. Secondly the foreground probability of each point is calculated. And then the probability threshold is set and processed by binary operation. And then the binary segmentation results are used to calculate the boundary of the pulmonary parenchyma segmentation. Finally, the pulmonary parenchyma is the original CT image with the binary segmentation result mask operation.

2.1. Selection of Seed Spots

In the random walk algorithm [11], the selection of seed points is of the utmost importance. In this experiment, we set the seed point as follows: one class called foreground seed, it refers to the seed point labeled in the pulmonary parenchyma; the other class is called the background seed point, it refers to all the areas except the pulmonary parenchyma , Including the heart, trachea, thorax and background areas. This method of using the artificial interaction of lung CT images of the pulmonary parenchyma segmentation method solves the complex problem of segmentation, and improves the accuracy of the segmentation.

Seed points of interactive setting and usage method:

① Setting the foreground seed color is blue, the background seed color is red;

②The left mouse button clicked is selected as the seed point of the selected foreground, the right key clicked is the seed point of the selected background, and any other key clicked is selected as the end seed point, and the subsequent program is run;

③ The position of foreground seed point was 1, and the position of background seed point was 0;

④ For the edge depression and the accuracy of segmentation, it is necessary to set the seed points several times.

2.2. Calculation of Foreground Probability

U Onoma D P, Ruan S, Gardin I, et al. [12] studied the 3D random walk based segmentation for lung tumor delineation in PET image. The idea of random walk algorithm, proposed by Grady L [13], is that the probability of each point is the weighted average of the corresponding probability of the surrounding four neighborhoods. The calculation process is shown in Fig.1: that is, for any point i, Probability is $p(i)$, w_{left} is the weight between i point and its left neighborhood point, and $p(i)_{left}$ is the foreground probability of the left neighborhood of point i, that is $(w_{left} + w_{up} + w_{right} + w_{down})\ p(i) = w_{left}\, p(i)_{left} + w_{up}\, p(i)_{up} + w_{right}\, p(i)_{right} + w_{down}\, p(i)_{down.}$ Where w_{left} is equal to $e^{-|I_i - I_{left}|\beta}$ so each point is the foreground probability: $X=A\backslash b$

$$\begin{matrix} \text{Non-seed point location} \\ \\ \text{Seed point location} \\ \\ \text{Non-seed point location} \end{matrix} \begin{bmatrix} \cdots\cdots -w_{left} \cdots\cdots -w_{up} \cdots\cdots \sum w \cdots\cdots -w_{down} \cdots\cdots -w_{right} \cdots\cdots \\ \cdots\cdots \\ \cdots\cdots -w_{left} \cdots\cdots -w_{up} \cdots\cdots \sum w+100 \cdots\cdots -w_{down} \cdots\cdots -w_{right} \cdots\cdots \\ \cdots\cdots \\ \cdots\cdots -w_{left} \cdots\cdots -w_{up} \cdots\cdots \sum w \cdots\cdots -w_{down} \cdots\cdots -w_{right} \cdots\cdots \end{bmatrix} \begin{bmatrix} x \\ x \\ x \\ x \\ x \end{bmatrix} = \begin{bmatrix} 0 \\ 0 \\ 100 \\ 0 \\ 0 \end{bmatrix}$$

A x = b

Fig. 1. Foreground probability calculation

2.3. Extraction of ROI in Lung

Through the preprocessing of CT images and segmentation of lung parenchyma, CT images have high recognition degree, and the experienced doctors can directly identify lung nodules. As the complex shape of the pulmonary nodules, texture features and other factors, so the early pulmonary nodules are difficult to be detected by doctors, there will be misdiagnosis and missed diagnosis of the phenomenon. Therefore, it is necessary to further analyze and deal with the lung parenchyma segmented.

Extraction of ROI from the lung parenchyma can make a more accurate judgment of the pulmonary nodules. The method of extracting ROI by artificial method is used to process the samples of lung parenchyma segmented, which reduces the computational complexity of the ROI texture feature, and the normalized pixel of the region of interest is 128 × 128.

3. Texture Feature Extraction of CT Image in Lung Based on Gray Level Co-occurrence Matrix

P Yang et al. [14] used gray co-occurrence matrix to extract features. The paper based on the gray level co-occurrence matrix algorithm analyzes the texture feature of ROI of lung CT images, the basic idea: the first the ROI extracted from lung parenchyma above is determined, and then a gray level co-occurrence matrix which has various gray level distribution information is established, and finally the texture feature parameters based on the matrix is extracted. Experimental results show that the algorithm is fast and effective.

3.1. Texture Features of Gray Level Co-occurrence Matrix

Walaa [15] studied content based medical image retrieval with texture content using gray level co-occurrence matrix and K-means clustering algorithms. The gray level co-occurrence matrix reflects the information of the image gray level distribution, which includes the synthetic of direction, local field and amplitude of variation. It refers to the probability of the occurrence of pixels with gray values g_1 and g_2 in the direction of with a distance of d, and the probability is denoted as $P(g_1, g_2, d, \theta)$.The elements in the co-occurrence matrix P[16, 17] are defined as formulas (1):

$$P(g_1, g_2; d, \theta) = \frac{\#\left\{\left[(x_1, y_1), (x_2, y_2)\right] \in S \mid f(x_1, y_1) = g_1 \,\&\, f(x_2, y_2) = g_2\right\}}{\#S} \tag{1}$$

Where g_1 and g_2 are gray values and S is the sum of the pixel pairs.

We can see from formula (1) that the P is normalized, in which the total number of pairs of pixels on the numerator is composed of pixel pairs with gray values g_1 and g_2From the definition of the gray level co-occurrence matrix, there are four main variables affecting the computational complexity, N is the size of the image, L is the gray level of the image, d is the distance, and θ is the direction.

Angular Second Moment W_1

$$W_1 = \sum_{g_1} \sum_{g_2} \left[P\left(g_1, g_2; d, \theta\right) \right]^2 \tag{2}$$

The Angular Second Moment [15, 18-19] reflects the uniformity and smoothness of the image distribution. When all $P(g_1, g_2, d, \theta)$ are equal or concentrated in the vicinity of the main diagonal, W_1 reaches the minimum, and the image is the smoothest.

Contrast W_2

$$W_2 = \sum_{g_1} \sum_{g_2} \left(g_1 - g_2\right)^2 P\left(g_1, g_2; d, \theta\right) \tag{3}$$

The Contrast [15, 18-19] reflects the amount of change in the local gray scale of the image, that is, the clarity of the image. When the small values in $P(g_1, g_2, d, \theta)$ are mainly concentrated in the vicinity of the main diagonal of the matrix, the larger the value of W_2 is, the greater the contrast of the pixels in the image is.

Inverse Difference Moment W_3

$$W_3 = \sum_{g_1} \sum_{g_2} \frac{P\left(g_1, g_2; d, \theta\right)}{1 + \left(g_1 - g_2\right)^2} \tag{4}$$

The uniformity can be regarded as the reciprocal of the Contrast to a certain extent. The closer the elements in the co-occurrence matrix $P(g_1, g_2, d, \theta)$are, the more similar they are, and the value of W_3 becomes larger and larger.

Entropy W_4

$$W_4 = -\sum_{g_1} \sum_{g_2} P\left(g_1, g_2; d, \theta\right) \lg P\left(g_1, g_2; d, \theta\right) \tag{5}$$

The Entropy [15, 18-21] reflects the inhomogeneity of texture, and if the probability of gray pairs between the pairs of pixels in the co-occurrence matrix is the same, then the entropy reaches the maximum.

Correlation W_5

$$W_5 = \frac{\sum_{g_1} \sum_{g_2} g_1 g_2 P\left(g_1, g_2; d, \theta\right) - \mu_x \mu_y}{\sigma_x \sigma_y} \tag{6}$$

Where $\mu_x, \mu_y, \sigma_x, \sigma_y$ are defined as:

$$\mu_x = \sum_{g_1} g_1 \sum_{g_2} P\left(g_1, g_2 : d, \theta\right) \tag{7}$$

$$\mu_y = \sum_{g_2} g_2 \sum_{g_1} P\left(g_1, g_2 : d, \theta\right) \tag{8}$$

$$\sigma_x^2 = \sum_{g_1} \left(g_1 - \mu_x\right)^2 \sum_{g_2} P\left(g_1, g_2 : d, \theta\right) \tag{9}$$

$$\sigma_y^2 = \sum_{g_2} \left(g_2 - \mu_y\right)^2 \sum_{g_1} P\left(g_1, g_2 : d, \theta\right) \tag{10}$$

The correlation coefficient [15, 18-19] reflects the linear correlation between the row and the column to a certain extent. When the correlation coefficient is larger, the gray level distribution of the image area is relatively uniform.

3.2. Analysis and Extraction of CT Image Texture Features in Lung

We know that there are four main variables affecting the computational complexity in the gray level co-occurrence matrix algorithm, namely, image size N, gray level L, distance d and direction θ. This algorithm analyzes the texture features of pulmonary nodules in lung CT images, and the following four variables are analyzed as follows.

Selection of image size N: The image is too small will lose part of the texture information, the image is too large to lead to storage and calculation is too large. In this paper, the size of the region of interest is set to $N = 128 \times 128$, and then the ROI region is transformed by some algorithm and the gray level of the region of interest is reduced to $L = 16$.

Selection of distance d: In the rough texture, the gray level co-occurrence matrix algorithm changes slowly under the influence of distance; in fine texture, the gray level co-occurrence matrix algorithm changes faster under the influence of distance. Experiments show that the distance $d = 1$ will get better results.

Selection of direction θ: The texture of the image has certain directionality, and the texture information of different co-occurrence matrix generated by different images is also different. A large number of experiments show that some texture information is incomplete, mainly because of the loss or abandonment of a direction of texture information, and generally use 0°, 45°, 90° and 135° directions to calculate the eigenvalues.

In this paper, based on the gray level co-occurrence matrix, the feature of the region of interest in the lung CT image is extracted. The extraction process is as follows:

① Read the region of interest;

② The gray level co-occurrence matrix of region of interest in 0°,45°,90° and 135° directions is calculated and normalized;

③ The normalized values in the direction of 0°, 45°, 90° and 135° are averaged;

④ Ten texture features of the mean and standard deviation of the Angular Second Moment W_1, the mean and standard deviation of the Contrast W_2, the mean and standard deviation of the Inverse Difference Moment W_3, the mean and standard deviation of the Sum of Entropy W_4, and the mean and standard deviation of the Correlation W_5 are calculated.

⑤ Save the eigenvalues to the database;

⑥ Calculate the next region of interest and return ①.

4. Recognition of Pulmonary Nodules Based on SVM

Rendon-Gonzalez E. et al. [22] performed automatic segmentation and classification of lung CT images based on support vector machines. In this paper, the feature vector of lung ROI is qualitatively classified based on support vector machine. The most important idea of support vector machine is to construct a maximum interval hyperplane based on the principle of structural risk minimization. Support vector machine algorithm can solve the problems of high dimension, small sample and data classification. The support vector machine has a certain dependence on the selection of kernel functions. Therefore,

choosing the appropriate kernel function and setting the optimal parameters is an important factor that directly affects the classification result. According to the result of the feature extraction, the linear kernel function is selected as the kernel function.

5. Experimental Results Analysis

5.1. Experimental Environment and Data

(1) Experimental environment: Matlab R2016b, LibSVM, Windows10 operating system.

(2) Experimental data:

Data source: 200 lung CT images marked by a doctor were used as experimental samples, of which 100 were pulmonary nodules and 100 were normal lungs.

Data preprocessing: because of the noise and artifacts of CT image, the first the image of CT image was denoised and enhanced, and the CT image information became clear and clear; then the size of CT image is normalized to 256 x 256. Finally, the 200 CT images were analyzed for pulmonary parenchyma, ROI extraction, feature extraction and SVM identification.

5.2. CT Image of Pulmonary Parenchymal Segmentation and ROI Extraction

Segmentation of pulmonary parenchyma in CT images is one of the important methods to deal with medical images. In this paper, the pulmonary parenchyma is segmented based on random walk algorithm, and the segmentation process is shown in Fig.2.

We can see from the process of segmentation of pulmonary parenchyma in Fig.2, (a) is the original image of the lung CT of the size of 255 × 255. Figure (b) is the selection of the seed point, the use of an interactive way to calibrate the foreground seed and background seed. In the figure (b), the region of the pulmonary parenchyma is labeled as the foreground seed (blue), and the region other than the pulmonary parenchyma is labeled as the background seed (red). Figure (c) Calculates the probability that each point belongs to the foreground based on the random walk algorithm. The random walk algorithm not only accurately distinguishes between two connected pulmonary parenchyma and two overlapping pulmonary parenchyma, but also has a good effect on the blurred question of the lung boundary and the disruption of the lung region. Figure (d) is the result of the binary segmentation. On the result of the calculation of foreground probability, the probability threshold is selected manually, and the threshold is set to 0.5. Figure (e) is the segmentation boundary of the pulmonary parenchyma, which is calculated from the probability threshold. Figure (f) is the result of segmentation of pulmonary parenchyma. Figure (f) is the result of segmentation of pulmonary parenchyma, which is the mask operation of figure (a) and figure (d).

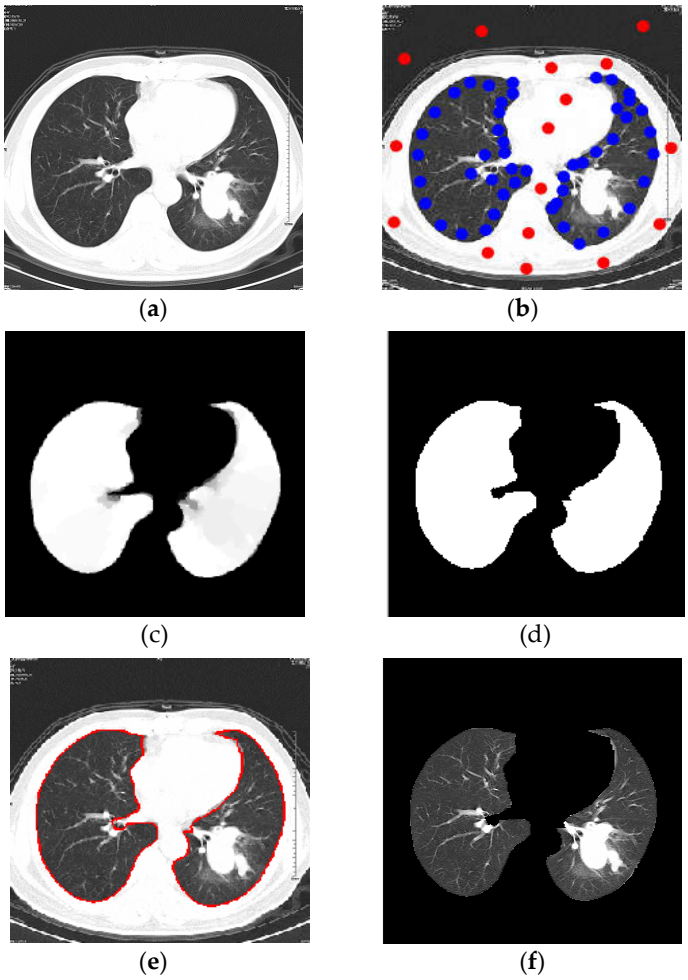

Fig. 2. This is pulmonary parenchymal segmentation process. (a) Original image; (b) Selection of seed point; (c) Calculation of foreground probability; (d) Binary segmentation results; (e) Segmentation boundary; (f) Segmentation result

ROI extraction is an important process to deal with medical images, it is the pulmonary parenchyma in the region of interest extracted. The extraction results are divided into two categories: pulmonary nodules and normal lung tissue. Fig.3 (a) gives four cases of pulmonary nodular CT images. Fig.3 (b) gives four cases of normal lung CT images.

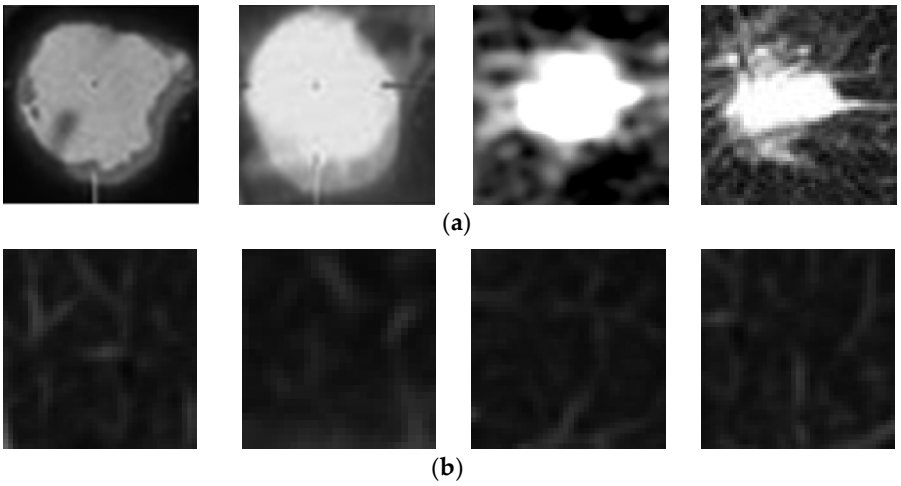

Fig. 3. This is partial lung CT images of ROI. (a) Pulmonary nodular CT image; (b) Normal lung CT image

Table 1. This is Partial sample texture feature extraction data (M – mean, SD – standard deviation)

category	Angular Second Moment		Entropy		Contrast		Inverse Difference Moment		Correlation	
	M	SD	M	SD	M	SD	M	SD	M	SD
1	0.402	0.018	1.367	0.088	0.113	0.043	0.957	0.015	1.117	0.029
1	0.354	0.019	1.526	0.108	0.134	0.054	0.951	0.018	1.058	0.033
1	0.465	0.018	1.271	0.087	0.118	0.043	0.957	0.015	1.780	0.090
1	0.380	0.016	1.228	0.072	0.067	0.025	0.968	0.012	2.153	0.070
1	0.385	0.015	1.527	0.094	0.166	0.063	0.954	0.016	0.718	0.021
1	0.543	0.013	1.195	0.074	0.105	0.046	0.968	0.012	0.814	0.020
1	0.498	0.016	0.933	0.057	0.053	0.019	0.974	0.010	3.194	0.119
1	0.583	0.015	0.957	0.062	0.057	0.021	0.972	0.010	2.913	0.115
1	0.593	0.014	0.917	0.056	0.051	0.018	0.975	0.009	3.596	0.147
0	0.112	0.009	2.728	0.145	0.326	0.147	0.927	0.027	0.049	0.001
0	0.229	0.006	2.433	0.134	0.519	0.241	0.930	0.026	0.055	0.003
0	0.048	0.007	3.370	0.163	0.276	0.102	0.883	0.037	0.064	0.001
0	0.079	0.005	3.075	0.148	0.219	0.092	0.914	0.031	0.036	0.000
0	0.104	0.005	2.935	0.132	0.211	0.086	0.919	0.028	0.030	0.002

0	0.149	0.010	2.421	0.090	0.228	0.061	0.896	0.024	0.148	0.006
0	0.107	0.005	2.955	0.145	0.251	0.109	0.917	0.030	0.029	0.003
0	0.237	0.011	2.290	0.120	0.270	0.101	0.914	0.027	0.098	0.002
0	0.130	0.010	2.663	0.146	0.361	0.153	0.907	0.031	0.056	0.001
0	0.156	0.006	2.475	0.108	0.131	0.050	0.943	0.021	0.070	0.007

5.3. Analysis of Texture Feature Extraction

The ROI was extracted from the segmented pulmonary parenchyma, and 200 samples with pulmonary nodules and normal lung tissue were obtained. The gray level co-occurrence matrix algorithm was used to extract the texture features of the samples from the pulmonary nodules and the normal lung tissue. Ten eigenvalues were calculated, which were the mean and standard deviation of the Angular Second Moment W_1, the mean and standard deviation of the Contrast W_2, the mean and standard deviation of the Inverse Difference Moment W_3, the mean and standard deviation of the Entropy W_4, and the mean and standard deviation of the Correlation W_5. In the category, 1 indicates pulmonary nodules, 0 indicates normal lung tissue, and part of the sample data is shown in Table1.

According to the data extracted from the texture features, 100 CT images with pulmonary nodules and 100 normal lung tissues were randomly selected. The eigenvalues of the Angular Second Moment and the Entropy were compared as shown in Fig.4. The feature curves of the Contrast and the Inverse Difference Moment are similar to those of the Entropy. Extraction of normal tissue and nodular features of the difference is more obvious.

The experimental results show that the texture feature extraction algorithm based on the gray level co-occurrence matrix is fast and feasible in the analysis of CT images of pulmonary nodules and normal lung tissues. When there is an obvious change in nodules in the lungs, the texture features between the normal lung tissue and the nodular texture features are quite different, and the texture of the image becomes rough. The experimental results also reflect that the extracted features can better distinguish nodules from pulmonary nodules and normal lung tissue, and provide good feature data for SVM classification.

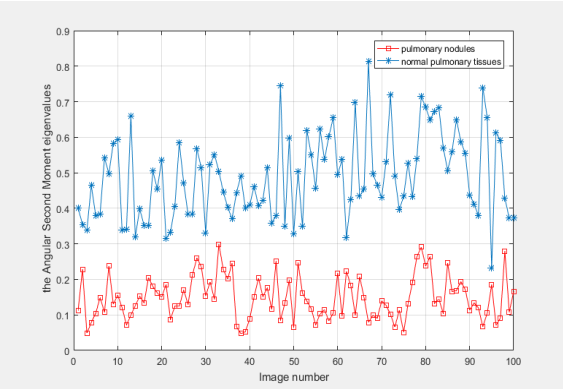

(a)

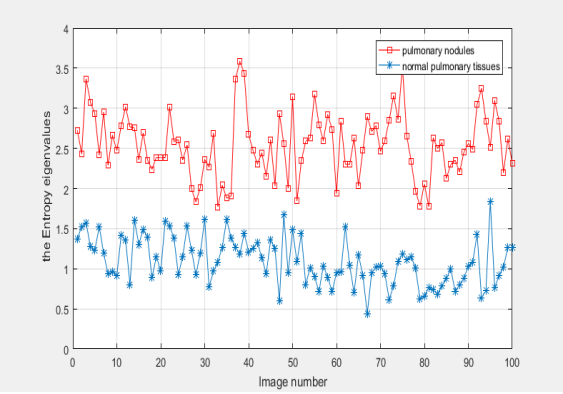

(b)

Fig. 4. (a) Comparison of the Angular Second Moment eigenvalues of CT images in pulmonary nodules and normal pulmonary tissues; (b) Comparison of the Entropy eigenvalues of CT images in pulmonary nodules and normal pulmonary tissues

5.4. Analysis of SVM Recognition Results

In this paper, support vector machine is used to classify pulmonary nodules, in which the kernel function is a linear kernel function. In the 3.2 section, ten dimensional feature vectors extracted from the region of interest of lung nodules are classified by support vector machine. After many experiments, the accuracy of recognition results is 94%, which proves the validity of the method. Therefore, the 2D training data were drawn showplot in MATLAB R2016b, the experimental results are shown in Fig.5 and Table 2.

The experimental results show that the accuracy of SVM classification based on random walk algorithm is significantly improved compared with fuzzy automatic seed cluster means morphological algorithm and Otsu algorithm. This indicates that the random walk algorithm is effective in the segmentation of lung parenchyma in this

paper, not only ensuring the integrity, accuracy and robustness of segmentation, but also improving the accuracy of classification.

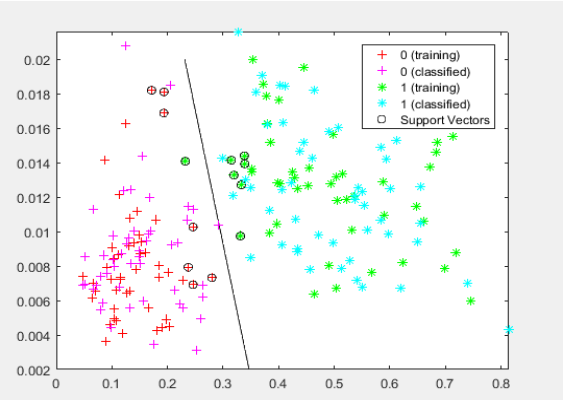

Fig. 5. This is classification results of pulmonary nodules

Table 2. This is Comparison based on SVM classification method

Author	Research methods			Accuracy rate
	Segmentation of pulmonary parenchyma	Feature extraction	Classification	
T Manikandan et al.[23]	Fuzzy auto-seed cluster means morphological algorithm	gray level co-occurrence matrix	SVM	93%
Antonio Oseas de Carvalho Filho et al.[24]	Otsu algorithm	Texture feature extraction	GA, SVM	92.52%
The proposed method	Random walk algorithm	gray level co-occurrence matrix	SVM	94%

6. Conclusions

In this paper, an auxiliary diagnosis method for automatic recognition of pulmonary nodules on lung CT images was proposed by correlation processing of lung CT images. The experimental results show that the pulmonary parenchymal segmentation in lung CT images is achieved based on the random walk algorithm, which has better effect on the blurred pulmonary boundary, the regional connectivity of the lungs and the overlapping of the lung parenchyma. In the process of extracting ROI from the lung parenchyma, the artificial extraction method has solved the extraction of ROI. Then, the feature of ROI was extracted based on the gray level co-occurrence matrix algorithm, that is, the mean

and standard deviation of the Angular Second Moment, the mean and standard deviation of the Contrast, the mean and standard deviation of the Inverse Difference Moment, the mean and standard deviation of the Entropy, and the mean and standard deviation of the Correlation, which are constructed a ten-dimensional feature vectors and finally formed a 200 × 10 matrix. Finally, the support vector machine algorithm is used to recognize pulmonary nodules. After many times of debugging and optimization, the recognition accuracy has reached above 94%. This method can help clinicians make diagnostic decisions quickly, accurately and efficiently.

Acknowledgments. This work is supported by the Harbin Science and Technology Bureau outstanding subject leader fund project (Project No.: 2017RAXXJ055), Harbin University of Commerce 2018 Graduate innovation research project (Project No.:YJSCX2018-526HSD), Harbin University of Commerce 2017 Graduate innovation research project (Project No.:YJSCX2017-441HSD) and 2016 young creative talent support project of Harbin University of Commerce (Project No.:2016QN051), Heilongjiang Provincial Fundamental Scientific Research Business Research Project (Project No.: 17XN003).

References

1. Torre L., Bray F., Siegel R., et al. Global cancer statistics, 2012: Global Cancer Statistics, 2012. Ca A Cancer Journal for Clinicians, Vol. 65, No. 2, 87-108. (2015)
2. Kwak E. L., Bang Y. J., Camidge D. R., et al. Anaplastic Lymphoma Kinase Inhibition in Non–Small-Cell Lung Cancer. New England Journal of Medicine, Vol. 363, No. 18, 1693-1703. (2010)
3. Al M. B., Brennan P. C., Mello-Thoms C. A review of lung cancer screening and the role of computer-aided detection. Clinical Radiology, Vol. 72, No. 6. (2017)
4. Liu S., Pan Z., Song H. Digital image watermarking method based on DCT and fractal encoding. Iet Image Processing, Vol. 11, No. 10, 815-821.(2017)
5. Liu S., Pan Z., Cheng X. A Novel Fast Fractal Image Compression Method based on Distance Clustering in High Dimensional Sphere Surface. Fractals-complex Geometry Patterns & Scaling in Nature & Society, Vol. 25, No. 23, 1740004. (2017)
6. Doi K. Computer-aided diagnosis in medical imaging: historical review, current status and future potential. Computerized Medical Imaging & Graphics, Vol. 31, No. 5, 198-211. (2007)
7. Kim B. C., Yu S. S., Suk H. I. Deep feature learning for pulmonary nodule classification in a lung CT. International Winter Conference on Brain-Computer Interface. IEEE, 1-3. (2016)
8. Kumar D., Wong A., Clausi D. A. Lung Nodule Classification Using Deep Features in CT Images. Conference on Computer and Robot Vision. IEEE Computer Society, 133-138. (2015)
9. Dhara A. K., Mukhopadhyay S., Dutta A., et al. A Combination of Shape and Texture Features for Classification of Pulmonary Nodules in Lung CT Images. Journal of Digital Imaging, Vol. 29, No. 4, 466-475. (2016)
10. Ozen Y., Kose C. Segmentation of lung CT images with random walk algorithm. Signal Processing and Communications Applications Conference. IEEE, 2206-2208. (2014)
11. Wang B., Xiaomeng G. U., Yang Y., et al. Automated lung segmentation for chest CT images based on Random Walk algorithm. Journal of Computer Applications. (2015)
12. Onoma D. P., Ruan S., Gardin I., et al. 3D random walk based segmentation for lung tumor delineation in PET imaging. IEEE International Symposium on Biomedical Imaging. IEEE, 1260-1263. (2012)

13. Grady L. Random Walks for Image Segmentation. IEEE Trans.pattern Anal.mach.intell, Vol. 28, No. 11, 1768-1783. (2006)
14. Yang P., Yang G. Feature extraction using dual-tree complex wavelet transform and gray level co-occurrence matrix. Neurocomputing, Vol. 197, No. C, 212-220. (2016)
15. Walaa. Content Based Medical Image Retrieval with Texture Content Using Gray Level Co-occurrence Matrix and K-Means Clustering Algorithms. Journal of Computer Science, Vol. 8, No. 7, 1070-1076. (2012)
16. Haralick R. M. Shanmugam K., Dinstein I. Textural Features for Image Classification. Systems Man & Cybernetics IEEE Transactions on, Vol. 3, No. 6, 610-621. (1973)
17. Partio M., Cramariuc B., Gabbouj M., et al. Rock texture retrieval using gray level co-occurrence matrix. Proc of Nordic Signal Processing Symposium Norsig Norway. (2002)
18. Park M., Wilson L. S., Wilson L. S. Detection of abnormal texture in chest X-rays with reduction of ribs. Pan-Sydney Area Workshop on Visual Information Processing. Australian Computer Society, Inc. 71-74. (2004)
19. Yin D., Pan J., Chen P., et al. Medical Image Categorization Based on Gaussian Mixture Model. International Conference on Biomedical Engineering and Informatics. IEEE, 128-131. (2008)
20. Liu S., Lu M., Liu G., et al. A Novel Distance Matric: Generalized Relative Entropy. (2017)
21. Liu S., Fu W., He L., et al. Distribution of primary additional errors in fractal encoding method. Multimedia Tools and Applications, Vol. 76, No. 4, 5787-5802. (2017)
22. Rendon-Gonzalez E., Ponomaryov V. Automatic Lung nodule segmentation and classification in CT images based on SVM. International Kharkiv Symposium on Physics and Engineering of Microwaves, Millimeter and Submillimeter Waves. IEEE, 1-4. (2016)
23. Manikandan T., Bharathi N. Lung Cancer Detection Using Fuzzy Auto-Seed Cluster Means Morphological Segmentation and SVM Classifier. Plenum Press. (2016)
24. Ao D. C. F., Silva A. C., Cardoso d P. A., et al. Computer-Aided Diagnosis of Lung Nodules in Computed Tomography by Using Phylogenetic Diversity, Genetic Algorithm, and SVM. Journal of Digital Imaging, Vol. 30, No. 6, 812-822. (2017)

Zhijie Zhao He was born in Harbin, China, in 1963. He is currently a professor at the School of Computer and Information Engineering at Harbin University of Commerce, China. He achieved his B. S. and M. S. Degree from Harbin University of Science and Technology, China, in 1985 and 1988 respectively, and obtained his PhD. from Harbin Institute of Technology in 2008. His research interests include image processing and intelligence information processing.

Cong Ren She received her B.S. degree from the School of Computer and Information Engineering at Harbin University of Commerce, China, in 2017. Currently, she is studying for her M.S. degree. Her research interests include image retrieval and intelligence information processing.

Huadong Sun He is currently an associate professor in the School of Computer and Information Engineering at Harbin University of Commerce, China. He obtained his B.S., M.S. and PhD. from Harbin Institute of Technology, China in 2002, 2004 and 2009, respectively. His research interests include image processing and intelligence information processing.

Zhipeng Fan He received M.S. degrees from the Harbin University of Commerce, Harbin, China. He is currently a lecturer with the School of computer and Information Engineering, Harbin University of Commerce. He has published a number of journal and conference papers in the field of video compression and image coding. His current research interests include intelligence information processing and business data analysis.

Ze Gao She received her B.S. degree from the School of Computer and Information Engineering at Harbin University of Commerce, China, in 2016. Currently, she is studying for her M.S. degree. Her research interests include image retrieval and intelligence information processing.

Received: October 20, 2017; Accepted: July 11, 2018.